

# The Effect of Blood Inflow and $B_1$ -field Inhomogeneity on Measurement of the AIF in Axial 3-D SPGR DCE-MRI

C. Roberts<sup>1,2</sup>, R. A. Little<sup>1,2</sup>, Y. Watson<sup>1,2</sup>, S. Zhao<sup>1,2</sup>, D. L. Buckley<sup>3</sup>, and G. J. Parker<sup>1,2</sup>

<sup>1</sup>Imaging Science and Biomedical Engineering, The University of Manchester, Manchester, United Kingdom, <sup>2</sup>The Biomedical Imaging Institute, The University of Manchester, Manchester, Greater Manchester, United Kingdom, <sup>3</sup>Division of Medical Physics, University of Leeds, Leeds, United Kingdom

**Introduction** Although there is a wide range of DCE-MRI protocols in the literature, the most commonly used 3-D dynamic contrast-enhanced MRI (DCE-MRI) acquisition is the 3-D spoiled gradient echo method (3D SPGR) (1), which is generally used to provide  $T_1$  estimates via the variable flip angle technique. A major potential confound in the context of a 3-D acquisition is the blood inflow effect and therefore the choice of slice location for arterial input function (AIF) measurement within the imaging volume must be considered carefully in order to minimize such error. Additionally, if confidence in the measurement of blood  $T_1$  is low, then an assumed value may be preferred. In this study, we use computer simulations, flow phantom and *in vivo* studies to describe and understand the effect of blood inflow on the measurement of the AIF in a typical 3-D axial DCE-MRI study scenario and consider the effects of assuming a blood  $T_1$  value on the measurement of the AIF and subsequent tracer kinetic parameterizations.

**Methods Imaging:** All imaging was performed using a 1.5T Philips Intera MR scanner (Best, Netherlands). A 3-D axial SPGR sequence was used and baseline  $T_1$  was estimated using variable flip angles of 2°, 10° and 20°, TR/TE = 4.0/1.02 ms, FOV = 165/375 mm<sup>2</sup> (phantom/*in vivo*), matrix = 128<sup>2</sup>, slices = 25, thickness = 4 mm. For the dynamic series, 45/75 (phantom/*in vivo*) sequential volumes with temporal resolution = 5 s (TR/TE/FOV identical, flip angle = 20°) were acquired during which time 0.5 mmol/ml gadodiamide (Omniscan, GE Healthcare) contrast agent (CA) was administered.

**Flow Phantom:** Imaging was performed on a pump-driven MR compatible flow apparatus which circulated Omniscan-doped water at a flow rate of 57 cm/s, which is comparable to aortic flow rates *in vivo*. During the dynamic series, a 1 ml bolus of contrast agent was administered at a rate of 2 ml/s. A region of interest was defined in the tubing on each axial slice of the volume and input functions were extracted. To measure the  $B_1$  efficiency, a 16-point  $B_1$  mapping sequence was also implemented using the same gradients, RF pulse shape, FOV, image geometry, with nominal flip angles of 0°, 150° and then every 15° increments to 360° (2). The effective flip angle ( $FA_{eff}$ ) after accounting for  $B_1$  variation was mapped at each slice.

**Computer Simulations:** We simulated the generation of the MR signal, and resulting baseline  $T_1$  measurement, in flowing blood using the same image sequence parameters (incorporating the effective flip angle determined from the  $B_1$  mapping sequence). AIFs were then simulated for each slice in the volume, using both our measured  $T_1$  and assumed  $T_1$  of 1.4 s (5). Additionally, to assess the effect of these AIFs on tracer kinetic modeling parameters, a tumor uptake curve with known values of  $K^{trans}$ ,  $v_e$  and  $v_p$  (0.1 min<sup>-1</sup>, 0.3 and 0.05 respectively) was simulated using the extended Kety model (3) and subsequently fit with all AIFs to give flow affected estimates of  $K^{trans}$ ,  $v_e$  and  $v_p$  derived from AIFs extracted at each slice in the volume.

**In-vivo DCE-MRI data:** 15 patients undertook 5 separate 3-D DCE-MRI scans (with the aorta running through all slices) on different occasions. During the dynamic series, 0.1 mmol/kg of body weight of contrast agent was administered through a Spectris power injector (Medrad Inc.) at a rate of 3 ml/s followed by an equal volume of saline flush also at 3 ml/s. AIFs were measured from each slice in the imaging volume using an automated method (4).

**Analysis:** For all experiments, signal intensity AIFs were converted to  $[CA](t)$  (mmol.kg<sup>-1</sup>) using the known SPGR relationship between signal and  $1/T_1(t)$  (1), where  $T_1(0)$  was either measured or assumed. For the latter,  $M_0$  was derived from the mean baseline signal intensity from the dynamic time series. For each AIF at each slice location the area under the AIF curve ( $AUC_{AIF}$ ) (units mmol.l<sup>-1</sup>.s) was computed using trapezoidal integration. All simulations and analysis was performed using MatLab (The MathWorks, Natick, Massachusetts, USA).

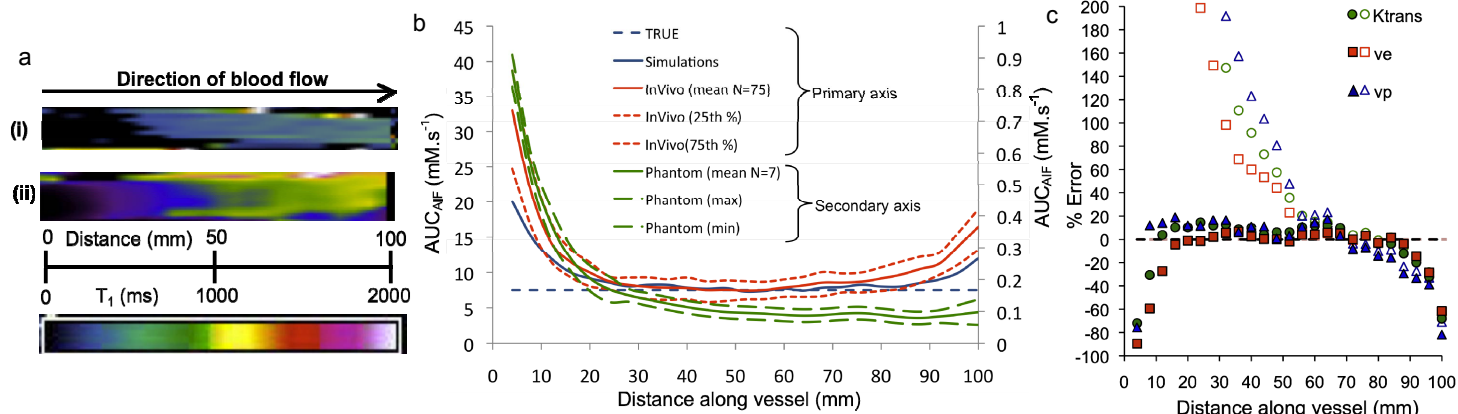


**Figure 1:** (a) Color-coded  $T_1$  maps of flowing "blood" within the phantom tubing (i) and an example aorta (ii) from our imaging volume. (b) Area under the measured AIF as a function of distance along the vessel for simulation, phantom and *in vivo* experiments. (c) % error in  $K^{trans}$ ,  $v_e$  and  $v_p$  derived using an AIF measured at different points along the vessel where baseline  $T_1$  was explicitly measured (closed symbols) or assumed as 1.4 s (open symbols).

**Results** The  $T_1$  measurements in flowing "blood" demonstrate vessel position-dependent errors in both the *in vivo* and flow phantom experiments (Fig. 1a). Measured AIFs along the vessel length from both *in vivo* and the flow phantom are in good agreement with simulated data and show  $[CA]$  elevations in the first 30 mm of the vessel, whereas AIFs measured from a more central slice position show  $[CA]$  measurements that match the 'true' AIF (Fig. 1b). Large errors in  $K^{trans}$ ,  $v_e$  and  $v_p$  are present at the volume extremities, which are accentuated by use of an assumed blood  $T_1$ .

**Discussion** This study has demonstrated that large errors in the measurement of the AIF (Fig. 1b) and thus estimations of tumor microvascular parameters occur over large parts of the imaging volume (Fig. 1c), emphasizing the need for careful placement of the AIF definition location. In a typical DCE-MRI study where RF inhomogeneity and blood inflow are left uncorrected, the resulting errors in flip angle and signal intensity are propagated through to estimates of  $T_1$  (Fig. 1a) and  $[CA]$ , as demonstrated in this study. Assumption of baseline blood  $T_1$  can lead to additional errors and therefore, if possible,  $T_1$  measurements that are robust to inflow measurements should be used for DCE-MRI. The blood inflow and  $B_1$  inhomogeneity effects we show on the measurement of the AIF should therefore be carefully considered in the context of a 3-D DCE-MRI study.

**References** 1. Li KL et al. J Magn Reson Imaging 2000;12(2):347-357. 2. Vaughan JT et al. Magn Reson Med 2001;46(1):24-30. 3. Tofts PS. J Magn Reson Imaging 1997;7(1):91-101. 4. Parker GJ et al. Magn Reson Med 2006;56(5):993-1000. 5. Stanisz G et al. Magn Reson Med 2005;54(3):507-512.